Cosmic Topology of Double Action Manifolds

R. Aurich and S. Lustig

Institut für Theoretische Physik, Universität Ulm,
Albert-Einstein-Allee 11, D-89069 Ulm, Germany

Abstract. The cosmic microwave background (CMB) anisotropies in spherical 3-spaces with a non-trivial topology are studied. This paper discusses the special class of the so-called double action manifolds, which are for the first time analysed with respect to their CMB anisotropies. The CMB anisotropies are computed for all double action manifolds generated by a dihedral and a cyclic group with a group order of up to 180 leading to 33 different topologies. Several spaces are found which show a suppression of the CMB anisotropies on large angular distances as it is found on the real CMB sky. It turns out that these spaces possess fundamental cells defined as Voronoi domains which are close to highly symmetric polyhedra like Platonic or Archimedean ones.

1. Introduction.

The NASA satellite COBE was not only the first mission which discovers fluctuations in the cosmic microwave background (CMB) radiation, but it also revealed that these fluctuations are almost uncorrelated at large angular scales [1]. This important observation was later substantiated by the WMAP mission [2], and it is described by the temperature 2-point correlation function

$$C(\vartheta) := \langle \delta T(\hat{n}) \delta T(\hat{n}') \rangle \quad \text{with} \quad \hat{n} \cdot \hat{n}' = \cos\vartheta \quad , \tag{1}$$

where $\delta T(\hat{n})$ is the temperature fluctuation in the direction of the unit vector $\hat{n}$. Since the correlations are most strongly suppressed at angles $\vartheta \gtrsim 60°$, the scalar measure

$$S := \int_{\cos(180°)}^{\cos(60°)} d\cos\vartheta \, |C(\vartheta)|^2 \tag{2}$$

is introduced in [2]. Small values of the S statistics signify a low correlation at large angles.

The observed low values of the S statistics cannot be easily reconciled with the cosmological ΛCDM concordance model. Among the suggested possibilities to explain this behaviour is that the spatial space might not be infinite as assumed by the

concordance model. The space could possess a non-trivial topology which can lead to multi-connected spaces with a finite volume. Due to the lower cutoff in their wavenumber spectrum $\{k\}$, these spaces can naturally explain the low correlations in the CMB sky. More details on the cosmic topology can be found in [3, 4, 5, 6, 7].

In this paper, it is assumed that the spatial space has a slight positive curvature, so that the simply-connected space is the spherical 3-space $\mathcal{S}^3$ which can be embedded in the four-dimensional Euclidean space as a 3-sphere

$$\vec{x} = (x_0, x_1, x_2, x_3)^T \in \mathcal{S}^3$$

together with the constraint $|\vec{x}|^2 = x_0^2 + x_1^2 + x_2^2 + x_3^2 = 1$. Using complex coordinates $z_1 := x_0 + \mathrm{i}x_3$ and $z_2 := x_1 + \mathrm{i}x_2$, the coordinate matrix u can be defined

$$u := \begin{pmatrix} z_1 & \mathrm{i}z_2 \\ \mathrm{i}\overline{z}_2 & \overline{z}_1 \end{pmatrix} \in \mathrm{SU}(2, \mathbb{C}) \equiv \mathcal{S}^3 \quad . \tag{3}$$

The advantage of the complex representation is that the transformations on $\mathcal{S}^3$ are determined by two $\mathrm{SU}(2, \mathbb{C})$ matrices denoted as the pair (g_a, g_b) that acts on the points $u \in \mathrm{SU}(2, \mathbb{C})$ of the 3-sphere $\mathcal{S}^3 \equiv \mathrm{SU}(2, \mathbb{C})$ by left and right multiplication

$$g := (g_a, g_b) : u \to g_a^{-1}\, u\, g_b \quad . \tag{4}$$

The points u and $g(u)$ are identified if g belongs to a deck group Γ. The 3-sphere $\mathcal{S}^3$ is tessellated in this way by a deck group Γ into as many domains as the deck group has elements that is the order $|\Gamma|$ of the deck group. The deck groups that lead to spherical multi-connected manifolds are discussed in [8].

In the following the focus is put on the double action manifolds that are generated by two finite subgroups R and L of Clifford translations. The defining property of Clifford translations is that all points u are translated by the same spherical distance. Furthermore, they can be divided into left- and right-handed Clifford translations depending on whether the flow lines spiral clockwise and anticlockwise around each other, respectively. In order to obtain a fix-point free group Γ, the two subgroups R and L have to fulfil some conditions [8]. It turns out that either R or L must be cyclic, and we take $L = Z_n$ as the cyclic subgroup of Clifford translations without loss of generality. The subgroup R is chosen as the binary dihedral group $D_p^\star$ where the group orders n and p must not have a common divisor greater than one.

The cyclic subgroup $L = Z_n$ of Clifford translations is generated by

$$g_{l1} = (\mathbf{1}, g_b) \quad \text{with} \quad g_b = \mathrm{diag}(e^{-2\pi\mathrm{i}/n}, e^{2\pi\mathrm{i}/n}) \quad , \tag{5}$$

since left-handed Clifford translations are realised by right multiplication. The other elements of L are obtained from (5) by

$$g_{lk} = \left(\mathbf{1}, (g_b)^k\right) \quad \text{for} \quad k = 1, \dots, n \quad . \tag{6}$$

The binary dihedral group $R = D_p^\star$ has the two generators $g_{r1} = (g_{a1}, \mathbf{1})$ and $g_{r2} = (g_{a2}, \mathbf{1})$ with

$$g_{a1} = \mathrm{diag}(e^{-\mathrm{i}\Psi_{az}}, e^{\mathrm{i}\Psi_{az}}) \quad \text{and} \quad g_{a2} = \begin{pmatrix} \cos(\Psi_{ay}) & -\sin(\Psi_{ay}) \\ \sin(\Psi_{ay}) & \cos(\Psi_{ay}) \end{pmatrix} \quad , \tag{7}$$

where $\Psi_{az} = 2\pi \left(\frac{2}{p}\right)$ and $\Psi_{ay} = 2\pi \left(\frac{1}{4}\right)$. The deck group Γ consists of all combinations of the elements of the subgroups R and L. The group order $|\Gamma|$ of the double action deck group is thus $|\Gamma| = n\,p$. In the following, the manifold generated by Γ is denoted as $DZ(p,n) := \mathcal{S}^3 / \left(D_p^\star \times Z_n\right)$ where the letters D and Z in $DZ(p,n)$ indicate the type of the group that is the binary dihedral and the cyclic group with group orders p and n, respectively.

2. Transforming the CMB Observer in Double Action Manifolds

Before we can proceed to the analysis of the CMB anisotropies of double action manifolds, we have to consider the transformation of the position $u \in \mathrm{SU}(2,\mathbb{C}) \equiv \mathcal{S}^3$ of the observer for which the CMB anisotropy is to be computed. Interestingly, it turns out that the statistical CMB properties depend on the observer position within the double action manifold.

The transformation is realised by applying an arbitrary isometry t to the coordinates

$$u \rightarrow u' = u\,t \;, \quad t \in \mathrm{SU}(2,\mathbb{C}) \quad . \tag{8}$$

Thus, the transformation is defined as right multiplication. Interpreting such a transformation as a shift of the origin of the coordinate system leads to a new representation of the group elements $g_k = (g_{ak}, g_{bk})$ of the deck group as

$$g_k' \;=\; (g_{ak}', g_{bk}') \;=\; (g_{ak}, t^{-1}\,g_{bk}\,t) \;, \quad k = 1, 2, \ldots, |\Gamma| \;, \tag{9}$$

as shown in [9, 10]. Thus, only the elements of the subgroup L are altered. The position dependence can conveniently be described by using the parameterisation

$$t(\rho, \alpha, \epsilon) \;=\; \begin{pmatrix} \cos(\rho)\,e^{+i\alpha} & i\sin(\rho)\,e^{+i\epsilon} \\ i\sin(\rho)\,e^{-i\epsilon} & \cos(\rho)\,e^{-i\alpha} \end{pmatrix} \tag{10}$$

for the transformation matrix t with $\rho \in [0, \frac{\pi}{2}]$, $\alpha, \epsilon \in [0, 2\pi]$. In this way the group elements g_k of Γ are functions of the parameters ρ, α, and ϵ.

3. Eigenmodes in Double Action Manifolds

Whether the dependence of the group elements $g \in \Gamma$ on the three parameters ρ, α, and ϵ carries over to the correlations in the CMB anisotropy or only a subset of them, characterises the deck group Γ and the multi-connected manifold. The statistical measures of the CMB are constructed rotationally invariant in order to obtain a measure that does not depend on the orientation of the coordinate system. Thus, if the transformation (9) leads to new group elements that can be considered as a pure rotation of the old ones, the CMB statistics does not change.

If there is no dependence of the CMB statistics on ρ, α, and ϵ at all, the manifold is called a homogeneous manifold. In this case, the CMB statistics does not depend on the observer position, and it suffices to analyse it for one representative position. In contrast, inhomogeneous manifolds possess observer position dependent CMB statistics,

and the CMB analysis requires a much more detailed investigation. In the case of the inhomogeneous lens spaces $L(p, q)$ which are studied in [11], there is only a ρ dependence, and the position dependent CMB analysis reduces to a one dimensional scan. This applies also to those inhomogeneous lens spaces which are coincidentally double action manifolds. It turns out, however, that the ensemble averages of the CMB properties of the double action manifolds $DZ(p, n)$ depend on two parameters, for which ρ and α are chosen. To show this, we need to discuss the Laplace-Beltrami operator Δ.

The eigenmodes of the Laplace-Beltrami operator Δ on the simply-connected spherical manifold $\mathcal{S}^3$ can be given as a product of the eigenmodes $|j_a, m_a\rangle$ and $|j_b, m_b\rangle$ of the abstract generators of the Lie algebra $\vec{J}_a = (J_{ax}, J_{ay}, J_{az}) \in \mathrm{SU}_a(2, \mathbb{C})$ and $\vec{J}_b = (J_{bx}, J_{by}, J_{bz}) \in \mathrm{SU}_b(2, \mathbb{C})$, respectively, for more details see [10]. Then, the complete set of eigenmodes for the eigenvalue $E_j := 4j(j+1) = (\beta^2 - 1)$ of the operator $-\Delta$ is obtained by

$$|j; m_a, m_b\rangle := |j, m_a\rangle |j, m_b\rangle \in \mathrm{SO}(4, \mathbb{R}) \quad . \tag{11}$$

In this notation the action of the generator (5) of the cyclic group Z_n is described by $U_{g_{l1}} = e^{\mathrm{i}(4\pi/n)J_{bz}}$. Analogously the action of the two generators (7) of the binary dihedral group $D_p^\star$ are given by $U_{g_{r1}} = e^{\mathrm{i}2\psi_{az}J_{az}}$ and $U_{g_{r2}} = e^{\mathrm{i}2\psi_{ay}J_{ay}}$ with ψ_{az} and ψ_{ay} defined below eq. (7). The eigenmodes on the manifold $DZ(p, n)$ have to be invariant under the action of $U_{g_{l1}}$, $U_{g_{r1}}$, and $U_{g_{r2}}$ [12], which is satisfied by

$$|j, i\rangle = \begin{cases} |j; m_a, m_b\rangle & : j \text{ even}, m_a = 0 \\ \frac{1}{\sqrt{2}} \left(|j; m_a, m_b\rangle + (-1)^{j+m_a} |j; -m_a, m_b\rangle \right) & : m_a > 0 \end{cases} \tag{12}$$

where $j \in \mathbb{N}_0 \setminus \{1, 3, ..., 2[\frac{p}{8}] - 1\}$, $m_b \in \mathbb{Z}$, $m_a \in \mathbb{N}_0$, $m_a \equiv 0 \bmod p/4$, $2\,m_b \equiv 0 \bmod n$ and $m_a, |m_b| \le j$. Here $i = i(m_a, m_b)$ with $1 \le i(m_a, m_b) \le r^{DZ(p,n)}(\beta)$ counts the multiplicity $r^{DZ(p,n)}(\beta)$ of the eigenvalue E_j. An analytic expression for this multiplicity is stated in table 1. This table also gives the multiplicity of the eigenvalue E_j for the double action manifolds $TZ(24, n) = \mathcal{S}^3 / (T^\star \times Z_n)$, $OZ(48, n) = \mathcal{S}^3 / (O^\star \times Z_n)$, and $IZ(120, n) = \mathcal{S}^3 / (I^\star \times Z_n)$, where $T^\star$, $O^\star$, and $I^\star$ are the binary tetrahedral, the binary octahedral, and the binary icosahedral group. The difference between these formulae of the double action manifolds and the expressions for the multiplicity of the corresponding homogeneous manifolds, see e.g. table 1 in [10], results from the additional constraint $2\,m_b \equiv 0 \bmod n$ due to the cyclic group Z_n. Therefore, the formulae for the multiplicity of the homogeneous manifolds are reproduced for $n = 1$.

$DZ(p, n)$ are inhomogeneous manifolds. For this reason the eigenmodes on the manifold $DZ(p, n)$ depend on the transformation to a new observer as discussed in section 2. The corresponding operator can be given by

$$D(t) = D(\alpha + \epsilon, 2\rho, \alpha - \epsilon) = e^{\mathrm{i}(\alpha+\epsilon)J_{bz}} e^{\mathrm{i}(2\rho)J_{by}} e^{\mathrm{i}(\alpha-\epsilon)J_{bz}} \quad , \tag{13}$$

where the coordinates (10) are used for the observer. For the following applications it is convenient to transform the eigenmodes $|j; m_a, m_b\rangle$ into the spherical basis $|j; l, m\rangle$, where l is the eigenvalue of $\vec{L} := \vec{J}_a + \vec{J}_b$. These two sets of eigenmodes are connected

manifold $\mathcal{M}$	wave number spectrum $\{\beta\}$	multiplicity $r^{\mathcal{M}}(\beta)$
$DZ(p,n)$, $p/4 \geq 2$ $\gcd(p,n)=1$	$\{1,5,9,\ldots,4\left[\frac{p}{8}\right]+1\}$ $\cup\{2k+1 \mid k \in \mathbb{N}, k \geq 2\left[\frac{p}{8}\right]+1\}$	$\left(\left[\frac{2(\beta-1)}{p}\right] + 2\left[\frac{\beta-1}{4}\right] - \frac{\beta-3}{2}\right)\left(2\left[\frac{\beta-1}{2n}\right]+1\right)$
$TZ(24,n)$ $\gcd(24,n)=1$	$\{1,7,9\}$ $\cup\{2k+1 \mid k \in \mathbb{N}, k \geq 6\}$	$\left(2\left[\frac{\beta-1}{6}\right] + \left[\frac{\beta-1}{4}\right] - \frac{\beta-3}{2}\right)\left(2\left[\frac{\beta-1}{2n}\right]+1\right)$
$OZ(48,n)$ $\gcd(48,n)=1$	$\{1,9,13,17,19,21\}$ $\cup\{2k+1 \mid k \in \mathbb{N}, k \geq 12\}$	$\left(\left[\frac{\beta-1}{8}\right] + \left[\frac{\beta-1}{6}\right] + \left[\frac{\beta-1}{4}\right] - \frac{\beta-3}{2}\right)\left(2\left[\frac{\beta-1}{2n}\right]+1\right)$
$IZ(120,n)$ $\gcd(120,n)=1$	$\{1,13,21,25,31,33,37\}$ $\cup\{41,43,45,49,51,53,55,57\}$ $\cup\{2k+1 \mid k \in \mathbb{N}, k \geq 30\}$	$\left(\left[\frac{\beta-1}{10}\right] + \left[\frac{\beta-1}{6}\right] + \left[\frac{\beta-1}{4}\right] - \frac{\beta-3}{2}\right)\left(2\left[\frac{\beta-1}{2n}\right]+1\right)$

Table 1. The spectrum of the eigenvalues $E_\beta = \beta^2 - 1$ of the Laplace-Beltrami operator on double action manifolds $\mathcal{M}$ and their multiplicities $r^{\mathcal{M}}(\beta)$ are given [12]. The bracket $[x]$ denotes the integer part of x.

by

$$|j;m_a,m_b\rangle = \sum_l \langle jm_a jm_b | lm\rangle \, |j;l,m\rangle \quad, \tag{14}$$

$$|j;l,m\rangle = \sum_{m_a} \langle jm_a jm_b | lm\rangle \, |j;m_a,m_b\rangle \quad,$$

where the $\langle jm_a jm_b | lm\rangle$ are the Clebsch-Gordan coefficients [13]. In general, $\langle jm_a jm_b | lm\rangle \neq 0$ only for $0 \leq l \leq 2j$ and $m_a + m_b = m$. Therefore, the expansion with respect to the spherical basis $|j;l,m\rangle$ of the eigenmodes $|j,i\rangle$, eq. (12), on $DZ(p,n)$ for an arbitrary observer results in

$$D(t^{-1})|j,i\rangle = \sum_{l=0}^{2j}\sum_{m=-l}^{l} \xi_{lm}^{j,i(m_a,m_b)}(DZ(p,n);t)\,|j;l,m\rangle \quad,$$

$$\xi_{lm}^{j,i(m_a,m_b)}(DZ(p,n);t)$$
$$= \begin{cases} \langle j0jm|lm\rangle\, D_{m,m_b}^j(t^{-1}) & : j \text{ even}, m_a = 0 \\ \frac{1}{\sqrt{2}}\Big(\langle jm_a jm-m_a|lm\rangle\, D_{m-m_a,m_b}^j(t^{-1}) \\ \quad + (-1)^{j+m_a}\langle jm_a jm+m_a|lm\rangle\, D_{m+m_a,m_b}^j(t^{-1})\Big) & : m_a > 0 \end{cases} \tag{15}$$

with $m_a \equiv 0 \bmod p/4$ and $2m_b \equiv 0 \bmod n$.

Here the definition of the Wigner polynomial

$$D_{\tilde{m}_b,m_b}^j(t) := \langle j,\tilde{m}_b | D(t) | j, m_b\rangle$$
$$= e^{\mathrm{i}(\alpha+\epsilon)\tilde{m}_b} d_{\tilde{m}_b,m_b}^j(2\rho) e^{\mathrm{i}(\alpha-\epsilon)m_b} \tag{16}$$

is used.

The calculation of the ensemble average of the temperature 2-point correlation function $C(\vartheta)$ or the multipole spectrum C_l on the manifolds $DZ(p,n)$ demands the computation of the quadratic sum of the expansion coefficients $\xi_{lm}^{j,i(m_a,m_b)}(DZ(p,n);t)$. This quadratic sum can be simplified:

$$\frac{1}{2l+1} \sum_{m=-l}^{l} \sum_{m_a,m_b} \left| \xi_{lm}^{j,i(m_a,m_b)}(DZ(p,n);t) \right|^2$$

$$= \frac{1}{2l+1} \sum_{m=-l}^{l} \left\{ \sum_{m_a,m_b} [\langle jm_a jm-m_a|lm\rangle \, d_{m-m_a,m_b}^{j}(-2\rho)]^2 \right. \tag{17}$$

$$+ \sum_{m_a>0,m_b} [(-1)^{j+m_a} \langle jm_a jm - m_a|lm\rangle \langle jm_a jm + m_a|lm\rangle$$

$$\left. d_{m-m_a,m_b}^{j}(-2\rho) \, d_{m+m_a,m_b}^{j}(-2\rho) \cos(2\,m_a\alpha)] \right\}$$

$$\text{with} \quad m_a \equiv 0 \bmod p/4 \quad \text{and} \quad 2\,m_b \equiv 0 \bmod n \quad .$$

This sum depends only on the coordinates ρ and α. Therefore, the analysis of the CMB statistics can be restricted to observer positions with $\epsilon = 0$. Furthermore, taking into account the condition $m_a \equiv 0 \bmod p/4$ and the symmetry of this sum with respect to the transformation $\rho \to \frac{\pi}{2} - \rho$, the domain of independent observer positions can be reduced to the smaller intervals $\alpha \in [0, \frac{\pi}{p}]$ and $\rho \in [0, \frac{\pi}{4}]$.

4. CMB Anisotropy on Large Angular Scales

The quadratic sum (17) of the expansion coefficients $\xi_{lm}^{j,i(m_a,m_b)}$ allows the computation of the ensemble average of the multipole moments C_l for the space $DZ(p,n)$

$$C_l := \frac{1}{2l+1} \sum_{m=-l}^{l} \langle |a_{lm}|^2 \rangle \tag{18}$$

$$= \sum_{\beta} \frac{T_l^2(\beta)\,P(\beta)}{2l+1} \sum_{m=-l}^{l} \sum_{i} \left| \xi_{lm}^{\beta,i}(DZ(p,n);t) \right|^2 \quad .$$

The initial power spectrum is $P(\beta) \sim 1/(E_\beta\,\beta^{2-n_{\rm s}})$ and $T_l^2(\beta)$ is the transfer function for which the same cosmological model as in [10] is used. After the multipole moments C_l have been obtained, the ensemble average of the 2-point correlation function $C(\vartheta)$ can be computed using

$$C(\vartheta) = \sum_{l} \frac{2l+1}{4\pi} C_l\,P_l\,(\cos\vartheta) \quad . \tag{19}$$

This in turn leads to the S statistics using eq. (2), and the extent of the suppression of the CMB correlations on large angular scales can be calculated. In the following, we always normalise the S statistics to that of the homogeneous $\mathcal{S}^3$ space. Thus, values of the S statistics below one indicate models that possess a stronger CMB suppression than that of the simply-connected spherical $\mathcal{S}^3$ space.
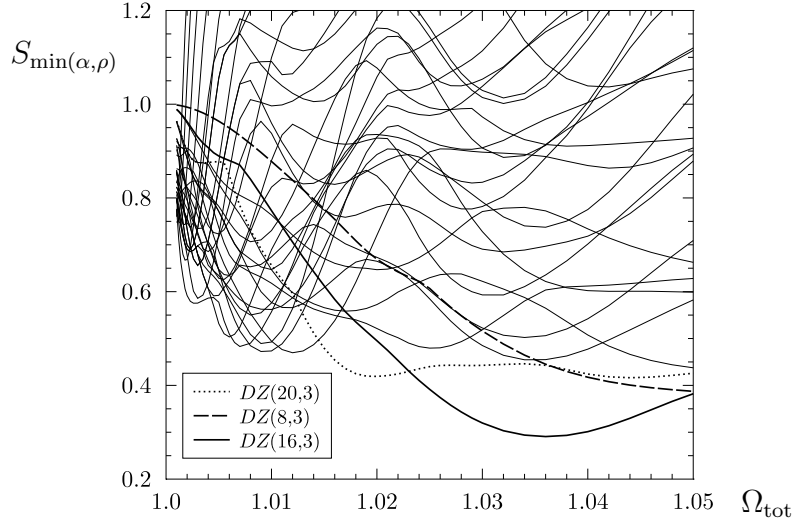
Figure 1. The minima of the S statistics, eq. (2), taken over all positions in the α-ρ plane, are plotted as a function of Ω_{tot} for all $DZ(p,n)$ spaces with $|\Gamma| = p\,n \leq 180$. The S statistics is normalised to that of the $\mathcal{S}^3$ space.

We compute the S statistics along these lines for sets of cosmological parameters which are close to the standard concordance model of cosmology ($\Omega_{\text{bar}} = 0.0485$, $\Omega_{\text{cdm}} = 0.238$, the Hubble constant $h = 0.681$). The density parameter of the cosmological constant Ω_Λ is varied such that the total density parameter Ω_{tot} is in the interval $\Omega_{\text{tot}} = 1.001, \ldots, 1.05$. Thus, we consider spherical models that are almost flat. For each value of Ω_{tot} the S statistics is calculated for numerous observer positions described by the parameters α and ρ. The values of α and ρ are obtained from a sufficiently dense rectangular mesh with $\alpha \in [0, \frac{\pi}{p}]$ and $\rho \in [0, \frac{\pi}{4}]$. This leads to almost 4.3 million simulations up to $\Omega_{\text{tot}} = 1.05$.

The minima of the S statistics

$$S_{\text{min}(\alpha,\rho)} = \min_{\{\alpha,\rho\}} \left(\frac{S(\alpha,\rho)}{S_{\mathcal{S}^3}} \right) \tag{20}$$

are determined for fixed values of Ω_{tot} for all 33 topologies $DZ(p,n)$ with a group order up to 180 and are plotted in figure 1. There are several spaces that have a CMB suppression more than two times stronger than in the $\mathcal{S}^3$ space. The $DZ(16,3)$ space has a minimum at $\Omega_{\text{tot}} = 1.036$ with $S_{\text{min}(\alpha,\rho)} = 0.291$. Thus it has three times smaller correlations compared to the $\mathcal{S}^3$ space. Another candidate is provided by the double action space $DZ(20,3)$ which has two almost equal minima at $\Omega_{\text{tot}} = 1.020$ and at $\Omega_{\text{tot}} = 1.044$. The minima are $S_{\text{min}(\alpha,\rho)} = 0.419$ and $S_{\text{min}(\alpha,\rho)} = 0.416$, respectively. Therefore, if one allows for Ω_{tot} only values as large as $\Omega_{\text{tot}} = 1.02$, the best candidate would be provided by the $DZ(20,3)$ space. If one restricts Ω_{tot} to even smaller values, that is, to even flatter models, then several other $DZ(p,n)$ spaces possess the lowest CMB correlations. With $\Omega_{\text{tot}} < 1.015$ one finds the four models $DZ(24,5)$, $DZ(24,7)$, $DZ(28,5)$, and $DZ(32,5)$, satisfying $S_{\text{min}(\alpha,\rho)} < 0.5$. The corresponding values of

$S_{\min(\alpha,\rho)}$ are given in table 2, where the parameters of the best models are listed for all 33 manifolds restricted to $\Omega_{\text{tot}} \leq 1.05$.

manifold $\mathcal{M}$	$S_{\min(\Omega_{\text{tot}},\alpha,\rho)}$	Ω_{tot}	ρ	α
$DZ(8,3)$	0.387	1.050	0.479	0.785
$DZ(8,5)$	0.647	1.020	0.393	0.000
$DZ(8,7)$	0.707	1.008	0.212	0.000
$DZ(8,9)$	0.723	1.005	0.620	0.060
$DZ(8,11)$	0.735	1.003	0.668	0.112
$DZ(8,13)$	0.737	1.002	0.770	0.224
$DZ(8,15)$	0.743	1.002	0.691	0.071
$DZ(8,17)$	0.745	1.001	0.738	0.150
$DZ(8,19)$	0.748	1.001	0.738	0.117
$DZ(8,21)$	0.760	1.001	0.738	0.117
$DZ(12,5)$	0.437	1.050	0.385	0.000
$DZ(12,7)$	0.599	1.050	0.369	0.000
$DZ(12,11)$	0.656	1.003	0.055	0.000
$DZ(12,13)$	0.690	1.002	0.047	0.349
$DZ(16,3)$	0.291	1.036	0.385	0.000
$DZ(16,5)$	0.480	1.025	0.408	0.393
$DZ(16,7)$	0.550	1.008	0.181	0.178
$DZ(16,9)$	0.626	1.006	0.086	0.000
$DZ(16,11)$	0.586	1.003	0.055	0.262
$DZ(20,3)$	0.416	1.044	0.393	0.314
$DZ(20,7)$	0.562	1.010	0.605	0.000
$DZ(20,9)$	0.591	1.005	0.149	0.035
$DZ(24,5)$	0.470	1.012	0.565	0.262
$DZ(24,7)$	0.489	1.009	0.605	0.262
$DZ(28,3)$	0.455	1.034	0.385	0.224
$DZ(28,5)$	0.472	1.009	0.589	0.000
$DZ(32,3)$	0.502	1.034	0.377	0.172
$DZ(32,5)$	0.483	1.007	0.613	0.196
$DZ(36,5)$	0.503	1.006	0.620	0.000
$DZ(40,3)$	0.685	1.032	0.385	0.157
$DZ(44,3)$	0.656	1.003	0.055	0.000
$DZ(52,3)$	0.690	1.002	0.047	0.121
$DZ(56,3)$	0.667	1.002	0.039	0.112

Table 2. For the 33 double action manifolds $DZ(p,n) = \mathcal{S}^3 / \left(D_p^\star \times Z_n \right)$ up to the group order $|\Gamma| = 180$, the models with the lowest CMB correlations on large angular scales are given. The parameters Ω_{tot}, ρ, and α specify the model which leads to a minimal value in the S statistics.
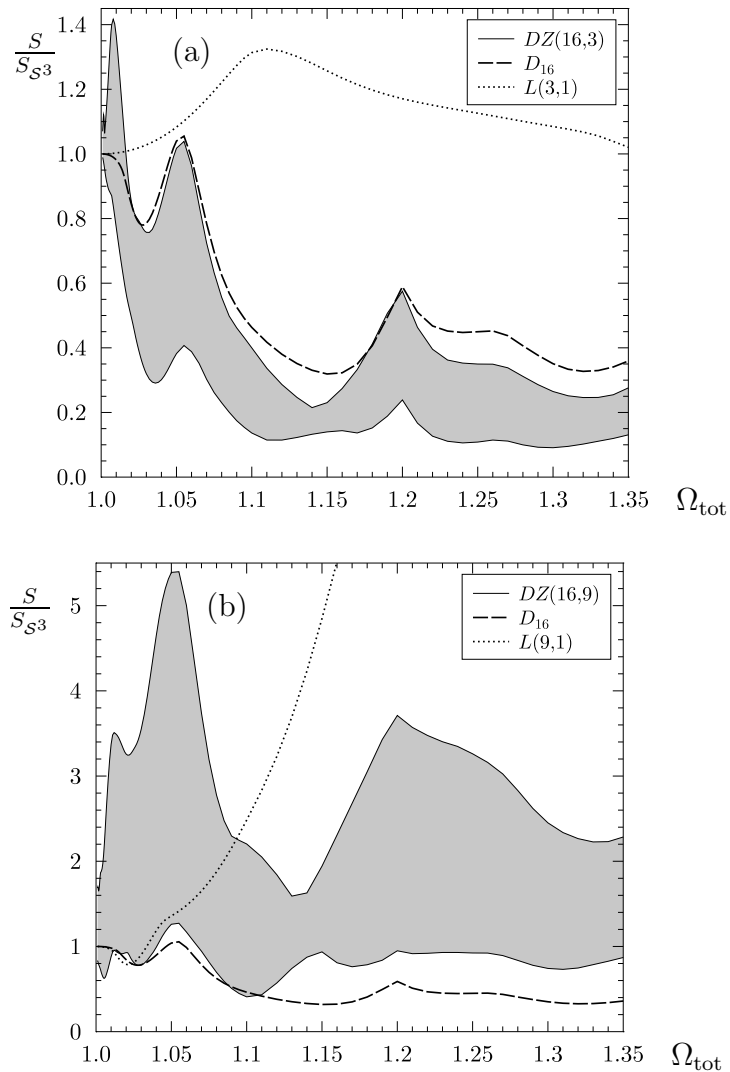
Figure 2. The panel (a) compares the S statistics of the homogeneous prism space D_{16} and the homogeneous lens space $L(3,1)$ with that of the inhomogeneous double action space $DZ(16,3)$. For the latter the variation of the S statistics due to the position dependence is shown as a grey band. It is obvious that the $DZ(16,3)$ space inherits its CMB properties from the D_{16} space but not from the lens space $L(3,1)$. The corresponding comparison of $DZ(16,9)$ with D_{16} and $L(9,1)$ is shown in panel (b). Note that both panels use a different scale and that the variation of the S statistics is much larger in the case $DZ(16,9)$.

The only manifold where the first minimum $S_{\min(\alpha,\rho)}$ lies outside this Ω_{tot} interval is $DZ(8,3)$ such that its value in table 2 is determined by this Ω_{tot} cut-off. The minimum with $S_{\min(\alpha,\rho)} = 0.060$ occurs at $\Omega_{\text{tot}} = 1.15$ with $\alpha = \rho = 0$. Although $DZ(8,3)$ has a very strong suppression, this value of Ω_{tot} is too large in order to be compatible with the current cosmological observations.

Let us discuss the favourite $DZ(16,3)$ in more detail. Since figure 1 only shows the minimum $S_{\min(\alpha,\rho)}$, the degree of variation with respect to the observer position
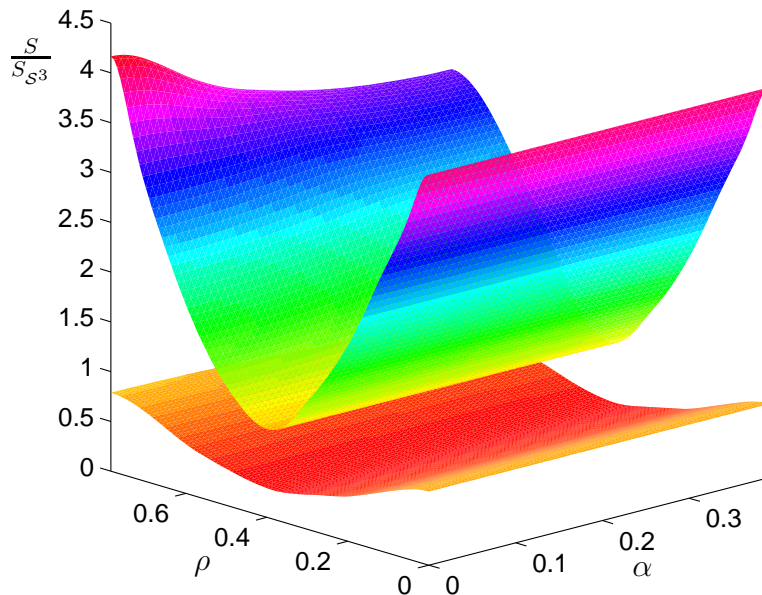
Figure 3. The normalised S statistics is shown in dependence on the observer position which is parameterised by ρ and α. The lower surface belongs to the double action space $DZ(16, 3)$ at $\Omega_{\text{tot}} = 1.036$. It has only a mild position dependence compared to the manifold $DZ(16, 9)$ (upper surface) computed for the same Ω_{tot}. The figure reveals that the position dependence is more pronounced with respect to the parameter ρ than to α in both cases.

parameterised by α and ρ is eliminated. This information is provided in figure 2(a) where the variation due to the position is shown as a grey band for the $DZ(16, 3)$ space. In addition, the panel shows the normalised S statistics of the homogeneous D_{16} and $L(3, 1)$ spaces (dashed and dotted curves) which are generated by the groups $D_{16}^\star$ and Z_3. Since $DZ(16, 3) = \mathcal{S}^3/(D_{16}^\star \times Z_3)$, these are the subgroups R and L generating $DZ(16, 3)$. The figure 2(a) reveals that it is the behaviour of the homogeneous D_{16} space which is responsible for the main behaviour of the inhomogeneous $DZ(16, 3)$. Because of this relevance for the $DZ(p, n)$ spaces, the table 3 lists the minima of their S statistics together with the value of Ω_{tot} where the minima occur. As in previous cases the Ω_{tot} interval is restricted to $\Omega_{\text{tot}} = 1.001 \ldots 1.05$. The table reveals that all prism spaces D_p, $p \le 72$, possess only a moderate suppression of large angle correlations below $\Omega_{\text{tot}} = 1.05$. The minimum for D_{16} at $\Omega_{\text{tot}} = 1.028$ can also be seen in figure 2 (dashed curves).

There are five manifolds $DZ(16, n)$ up to group order 180 which have the group $D_{16}^\star$ as a subgroup. As a further example the variation due to the observer position in $DZ(16, 9)$ is shown in figure 2(b) where the variation is larger than for the manifold $DZ(16, 3)$. The increased variability can be understood in terms of the number of inhomogeneous translations within the deck group. An inhomogeneous group element transforms different points $\vec{x} \in \mathcal{S}^3$ to varying spherical distances. This contrasts to

manifold $\mathcal{M}$	$S_{\min(\Omega_{\text{tot}})}$	Ω_{tot}
D_8	0.988	1.050
D_{12}	0.684	1.050
D_{16}	0.780	1.028
D_{20}	0.806	1.017
D_{24}	0.822	1.012
D_{28}	0.831	1.008
D_{32}	0.838	1.007
D_{36}	0.842	1.005
D_{40}	0.846	1.004
D_{44}	0.852	1.004
D_{48}	0.854	1.003
D_{52}	0.854	1.002
D_{56}	0.855	1.002
D_{60}	0.857	1.002
D_{64}	0.858	1.002
D_{68}	0.859	1.001
D_{72}	0.860	1.001

Table 3. The lowest CMB correlations on large angular scales $S_{\min(\Omega_{\text{tot}})}$ are given with the corresponding Ω_{tot} for all prism spaces D_p generated by the binary dihedral groups $D_p^\star$ up to the group order $|\Gamma| = p = 72$. The minima are determined for the interval $\Omega_{\text{tot}} = 1.001 \ldots 1.05$. The prism spaces are homogeneous, and thus an observer position is not required in this table.

Clifford transformations where all points $\vec{x} \in \mathcal{S}^3$ are shifted by the same spherical distance. The deck group of the manifold $DZ(16,3)$ contains 30 inhomogeneous transformations and 18 Clifford transformations. The number of inhomogeneous translations increases to 120 for the manifold $DZ(16,9)$. The large variability of the S statistics can be explained by this large number, since the CMB dependence on the observer position is the more pronounced, the more inhomogeneous translations are in the deck group. Conversely, the variation width must shrink to zero if all group elements are Clifford transformations whose transformation properties are independent of $\vec{x} \in \mathcal{S}^3$. To emphasise this point figure 3 displays the observer position dependence for the manifolds $DZ(16,3)$ and $DZ(16,9)$ of the normalised S statistics computed at the same value of $\Omega_{\text{tot}} = 1.036$. It is clearly seen that the $DZ(16,9)$ space has a severe position dependence compared to the space $DZ(16,3)$. Furthermore, both models posses only a modest variation with respect the the parameter α. Thus, the main variation is due to an observer shift in the ρ direction.
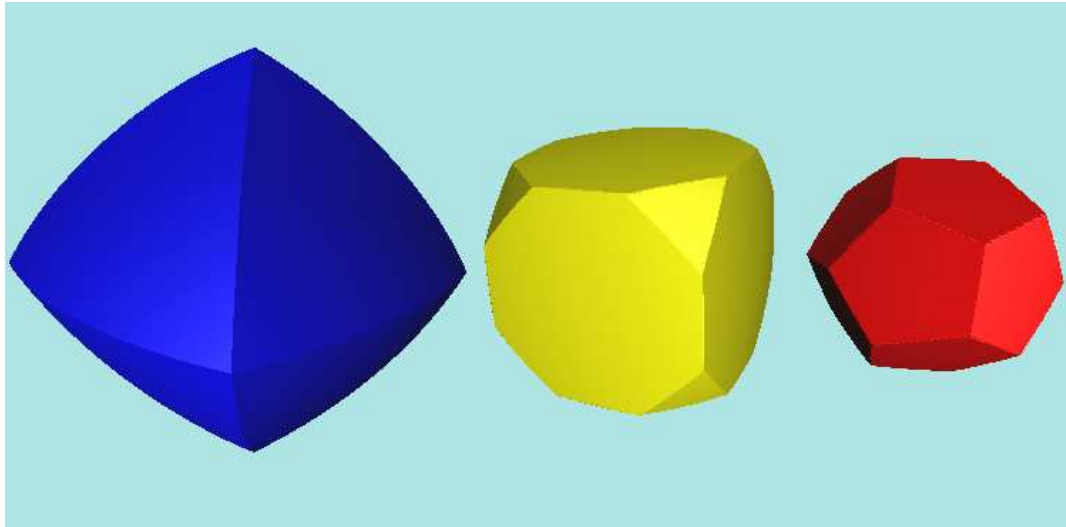
Figure 4. The Voronoi domains generated by the binary tetrahedral group $T^\star$ (blue), the binary octahedral group $O^\star$ (yellow), and the binary icosahedral group $I^\star$ (red) are shown. These three regular polyhedral spaces are homogeneous manifolds.

5. The shape of the Voronoi domains

As described in section 2 the representation of the group elements of the deck group Γ changes according to eq. (9). As a consequence the Voronoi domain alters due to shifts of the observer position. The Voronoi domain $\mathcal{F}$ is defined as the set of points $u \in \mathcal{S}^3$ that cannot be transformed any closer to the observer u_o by applying the elements of the deck group Γ, i.e.

$$u \in \mathcal{F} \quad \text{if} \quad d(u_o, u) \ \leq \ d(u_o, g(u)) \quad \text{for all } g \in \Gamma \quad , \tag{21}$$

where $d(u_1, u_2)$ measures the spherical distances between the points $u_1, u_2 \in \mathcal{S}^3$. It is instructive to compare the shape of the Voronoi domains at the positions of the observer where the values for the S statistics are extremal. The figure 4 shows the Voronoi domains of the spherical regular polyhedral spaces generated by the binary tetrahedral group $T^\star$, the binary octahedral group $O^\star$, and the binary icosahedral group $I^\star$ which are introduced in section 3. These groups consist only of Clifford transformations, so that the Voronoi domains are independent of the observer position, i.e. these manifolds are homogeneous.

Let us now turn to the $DZ(8,3)$ space which has its first minimum in the S statistics at $\Omega_{\text{tot}} = 1.15$. Figure 1 shows its behaviour up to $\Omega_{\text{tot}} = 1.05$ and the decline towards higher Ω_{tot} is already visible. In the range $\Omega_{\text{tot}} = 1.025 \ldots 1.065$ the minimum in the S statistics is achieved at $\rho = 0.479$ and $\alpha = \frac{\pi}{4}$ whereas the maximum occurs at $\rho = 0$ and $\alpha = 0$. The Voronoi domains for these positions are shown in figure 5. Interestingly, the orientations are reversed at the actual minimum at $\Omega_{\text{tot}} = 1.15$, i.e. the minimum occurs at $\rho = 0$ and $\alpha = 0$ and the maximum at $\rho = 0.479$ and $\alpha = \frac{\pi}{4}$. A further interesting
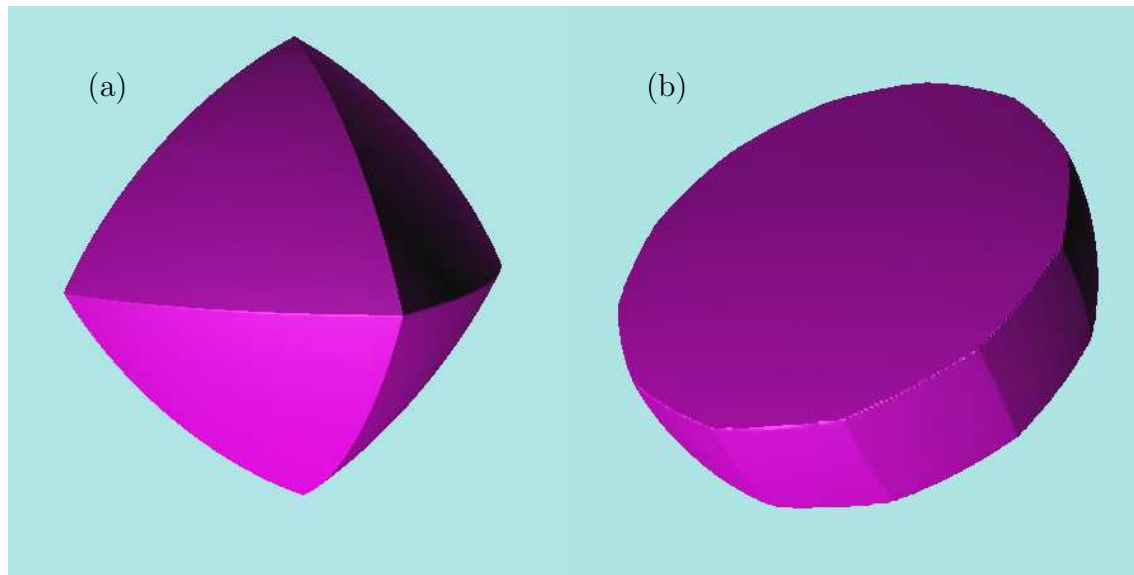
Figure 5. The Voronoi domains for $DZ(8,3)$ are shown with $\rho = 0.479$ and $\alpha = \frac{\pi}{4}$ in panel (a) and with $\rho = 0$ and $\alpha = 0$ in panel (b).

point is that the Voronoi domain of $DZ(8,3)$ is at $\rho = \frac{1}{2}\arccos(1/\sqrt{3}) \simeq 0.479$ and $\alpha = \frac{\pi}{4}$ identical to that of the binary tetrahedral space $\mathcal{T}$ shown in figure 4. This is remarkable in view of the so-called well-proportioned conjecture [14] which states that the CMB suppression on large angular scales is the more pronounced, the more well-proportioned the Voronoi domain is. Thus, one would expect the position at $\rho = 0.479$ and $\alpha = \frac{\pi}{4}$ always to be the one with the minimum in the S statistics. This provides therefore a counterexample to the conjecture. We would like to clarify that although the Voronoi domains of the binary tetrahedral space $\mathcal{T}$ and of the $DZ(8,3)$ space at $\rho = \frac{1}{2}\arccos(1/\sqrt{3})$ and $\alpha = \frac{\pi}{4}$ are identical, they nevertheless belong to different spaces since the gluing rules, which describe how to connect the faces, are different.

The discussion in section 4 shows that a very interesting double action space is provided by $DZ(16,3)$ having a strong CMB anisotropy suppression at $\Omega_{\mathrm{tot}} = 1.036$. The Voronoi domain for the observer who sees the minimal CMB anisotropy, i.e. $\rho = 0.385$ and $\alpha = 0$, is depicted in figure 6(a). A comparison with figure 4 reveals the similarity with the homogeneous space generated by the binary octahedral group $O^\star$. The Voronoi domain that exactly matches that of the binary octahedral group $O^\star$ occurs in $DZ(16,3)$ at $\rho = \frac{1}{2}\arccos(1/\sqrt{3}) \simeq 0.479$ and $\alpha = 0$. At this position the value for the S statistics is $S = 0.346$ which is larger than the minimal value $S = 0.291$ as revealed by table 2. Therefore, although both Voronoi domains are similar, the deviation demonstrates that the best Voronoi domain with respect to maximal CMB suppression is not the one with the most well-proportioned fundamental cell. Figure 6(b) shows the Voronoi domain of $DZ(16,3)$ at $\rho = \frac{\pi}{4}$ and $\alpha = 0$ which corresponds to the observer seeing the largest CMB anisotropy power on large angular scales at $\Omega_{\mathrm{tot}} = 1.036$.
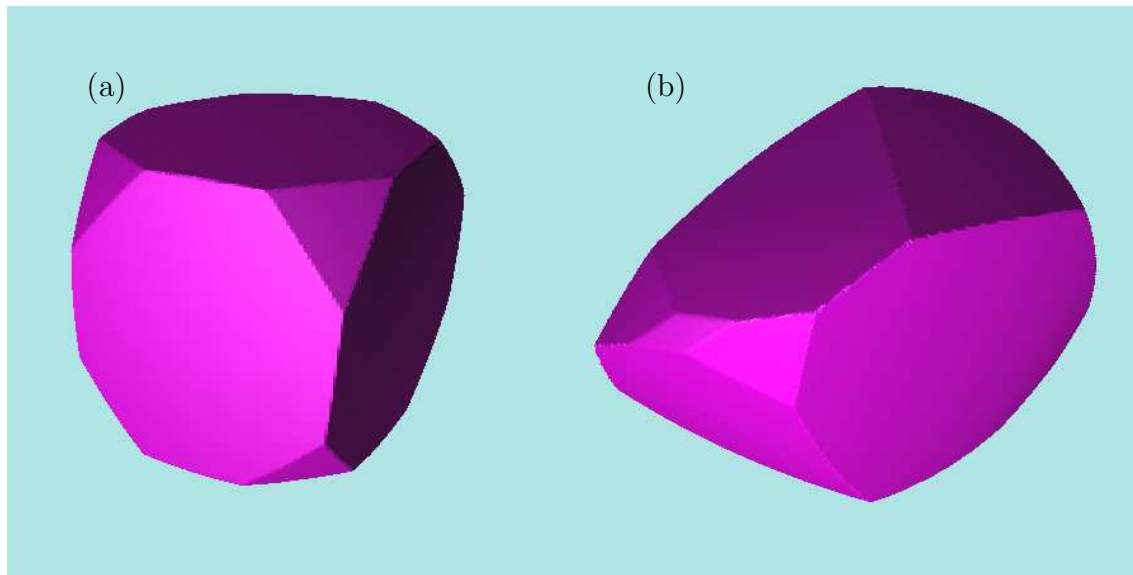
Figure 6. The Voronoi domains for $DZ(16,3)$ are shown with $\rho = 0.385$ and $\alpha = 0$ in panel (a) and with $\rho = \frac{\pi}{4}$ and $\alpha = 0$ in panel (b).

In section 4 it was shown that a much stronger observer-position dependence with respect to the S statistics occurs in $DZ(16,9)$ compared to $DZ(16,3)$. The $DZ(16,9)$ possesses a first minimum in the S statistics at $\Omega_{\text{tot}} = 1.006$ for the observer at $\rho = 0.086$ and $\alpha = 0$. At this value of Ω_{tot} the maximal CMB anisotropy even exceeds that of the simply-connected $\mathcal{S}^3$ space for an observer at $\rho = \frac{\pi}{4}$ and $\alpha = 0$. Figure 7 shows for both positions the corresponding Voronoi domains emphasising that the large variability in the S statistics is also reflected in the Voronoi domains. The $DZ(16,9)$ space cannot have a Voronoi domain corresponding to regular polyhedral spaces as shown in figure 4 since the group orders do not match.

Although deviations from the predictions of the well-proportioned conjecture are found, it is nevertheless remarkable that the Voronoi domains of two regular polyhedral spaces play a role with respect to the CMB anisotropy suppressions in double action manifolds $DZ(p,n) = \mathcal{S}^3 / \left(D_p^\star \times Z_n\right)$.

6. Comparison of Double Action Manifolds with Observations

Up to now the power of the correlation function for the manifolds $DZ(p,n)$ on scales larger than $60°$ is studied without reference to observations. In this section the correlations of the CMB for these models are compared with that of the WMAP 7yr data on all angular scales $\vartheta \in [0°, 180°]$ using the correlation function of the ILC 7yr map [15]. The integrated weighted temperature correlation difference [16]

$$I := \int_{-1}^{1} d\cos\vartheta \; \frac{(C^{\text{model}}(\vartheta) - C^{\text{obs}}(\vartheta))^2}{\text{Var}(C^{\text{model}}(\vartheta))} \tag{22}$$
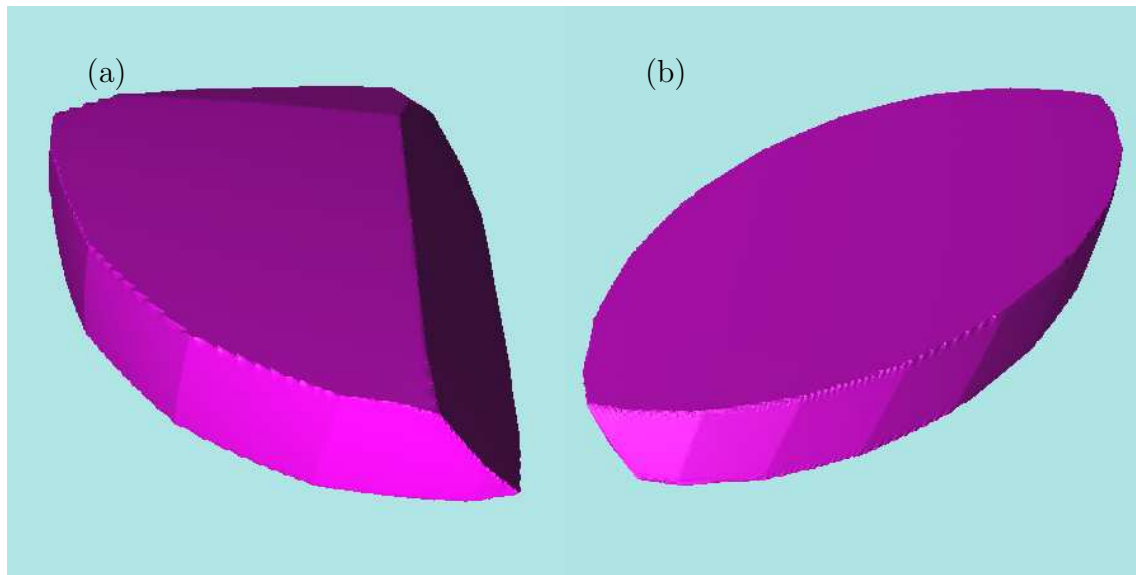
Figure 7. The Voronoi domains for $DZ(16, 9)$ are shown with $\rho = 0.086$ and $\alpha = 0$ in panel (a) and with $\rho = \frac{\pi}{4}$ and $\alpha = 0$ in panel (b).

is suited for such a comparison of the observed correlation function $C^{\mathrm{obs}}(\vartheta)$ with that of the model $C^{\mathrm{model}}(\vartheta)$, where the ensemble average due to the Gaussian initial condition is used for the latter. Furthermore, the model is normalised to the angular power spectrum of the WMAP data using the multipoles between $l = 20$ and 45. The cosmic variance of the model is computed using

$$\mathrm{Var}(C(\vartheta)) \approx \sum_l \frac{2l + 1}{8\pi^2} \left[C_l \, P_l(\cos \vartheta) \right]^2 \quad . \tag{23}$$

The I statistics is calculated for three different correlation functions $C^{\mathrm{obs}}(\vartheta)$ which are resulting in all three cases from the ILC 7yr map of the WMAP data but are based on different subsets of pixels. One correlation function $C^{\mathrm{obs}}(\vartheta)$ is obtained from the complete ILC 7yr map but the other two apply the KQ75 7yr and KQ85 7yr masks. The two masks are provided by [15], where the KQ85 7yr and the KQ75 7yr masks include 78.3% and 70.3% of the sky, respectively. For a discussion to this topic see e. g. [10].

The values of the I statistics are computed for all 33 double action manifolds $DZ(p, n)$ up to the group order $|\Gamma| = 180$ for the same values of Ω_{tot}, α, and ρ as in the previous sections. For a given manifold the best value for the I statistics, i. e.

$$I_{\min(\alpha, \rho, \Omega_{\mathrm{tot}})} = \min_{\{\alpha, \rho, \Omega_{\mathrm{tot}}\}} I(\alpha, \rho, \Omega_{\mathrm{tot}}) \quad , \tag{24}$$

is then determined where the Ω_{tot} interval is restricted to $\Omega_{\mathrm{tot}} \in [1.001, 1.05]$. These values are plotted as full disks in figure 8 where the three panels refer to the three different observational correlation functions $C^{\mathrm{obs}}(\vartheta)$. A survey of lens spaces $L(p, q)$ is provided in [11] where the S statistics as well as the I statistics are analysed for all
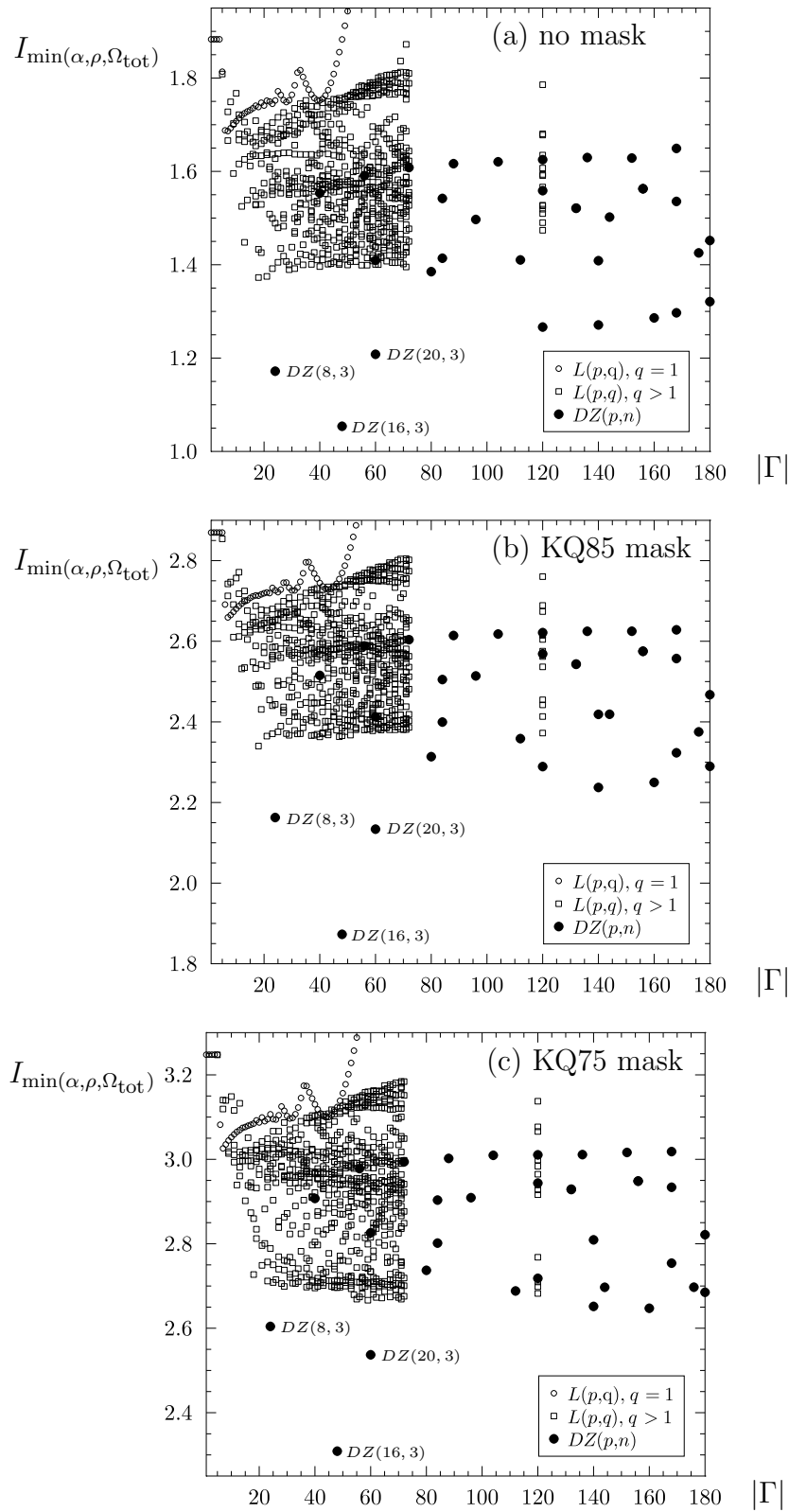
Figure 8. The minima of the I statistics taken over α, ρ, and Ω_{tot} are plotted for the double action manifolds $DZ(p, n)$ as full disks. The open circles and open boxes represent the homogeneous and inhomogeneous lens spaces $L(p, q)$. These are complete for $p \leq 72$ and, in addition, the group order $p = 120$ is also shown. The Ω_{tot} interval is restricted for both space classes to $\Omega_{\text{tot}} \in [1.001, 1.05]$.

lens spaces $L(p, q)$ up to the group order $p = 72$. It is found that two sequences of lens spaces exist with a relatively strong CMB anisotropy suppression. These data are also shown in figure 8 where the I statistics of these lens spaces is plotted as open circles for the homogeneous spaces $L(p, 1)$ (no minima has to be searched) and as open squares for the inhomogeneous spaces $L(p, q)$, $q > 1$. Three $DZ(p, n)$ spaces immediately attract attention because their values of the I statistics are significantly smaller than in any of the lens spaces $L(p, q)$. These three spaces are $DZ(16, 3)$, $DZ(8, 3)$, and $DZ(20, 3)$. The double action manifold $DZ(16, 3)$ leads to the best match for all three observational correlation functions $C^{\mathrm{obs}}(\vartheta)$, that is with the KQ75 7yr or KQ85 7yr mask or without a mask at all. The two other spaces change the second and third position with respect to the lowest value of $I_{\min(\alpha, \rho, \Omega_{\mathrm{tot}})}$ depending on the selected pixels of the ILC map. Using the KQ75 7yr or KQ85 7yr mask the space $DZ(20, 3)$ provides a slightly better description of the CMB data than $DZ(8, 3)$. This relation reverses if no mask is applied.

This comparison reveals that the three double action manifolds $DZ(16, 3)$, $DZ(8, 3)$, and $DZ(20, 3)$ produce the lowest CMB correlations among the two classes of inhomogeneous spaces $DZ(p, n)$ and $L(p, q)$.

7. Summary and Discussion

This paper studies whether a special class of spherical topologies can alleviate the apparent disagreement between the standard concordance model of cosmology and measurements of the low power at large scales in the cosmic microwave background maps. The cosmological observations point to an almost spatially flat cosmos. Thus, we restrict the analysis to spherical models that are almost flat by confining the total density parameter Ω_{tot} to the interval $\Omega_{\mathrm{tot}} = 1.001, \ldots, 1.05$. The space of such cosmological models is the simply-connected 3-sphere $\mathcal{S}^3$ if the model should be close to the concordance model. These concordance-like models produce, however, more correlations in the CMB temperature fluctuations on large angular scales as observed in CMB sky. This disagreement can be alleviated by considering instead of the simply-connected 3-sphere $\mathcal{S}^3$ a multi-connected space $\mathcal{M} = \mathcal{S}^3/\Gamma$ which is obtained from the 3-sphere $\mathcal{S}^3$ by tessellating it under the action of a deck group Γ.

Multi-connected spherical spaces can be classified into several groups, see e.g. [8]. On the one hand there a three deck groups which lead to regular polyhedral spaces. These are obtained by applying the binary tetrahedral group $T^\star$, the binary octahedral group $O^\star$, or the binary icosahedral group $I^\star$ to the 3-sphere $\mathcal{S}^3$. The polyhedral spaces are homogeneous in the sense that their fundamental domains defined as a Voronoi domain look the same independent of the position of the CMB observer. The important implication thereof is that the statistical CMB properties do not depend on the CMB observer. Manifolds which possess such a dependence are called inhomogeneous. It turns out that the regular polyhedral spaces yield CMB anisotropies with a normalised S statistics, eq. (2), of $S/S_{\mathcal{S}^3} \simeq 0.11$. This is the strongest suppression of CMB correlations on large angles found so far.

In addition to these three manifolds there are the so-called prism spaces, which are generated by the binary dihedral group $D_p^\star$. The prism spaces are homogeneous and are analysed up to the group order $p = 72$ in [10], see also [12]. The CMB suppression of some prism spaces can be as low as $S/S_{\mathcal{S}^3} \simeq 0.8 \ldots 0.9$ for $\Omega_\text{tot} = 1.001, \ldots, 1.05$ as shown in table 3. The prism space D_{12} drops even to $S/S_{\mathcal{S}^3} \simeq 0.68$ at $\Omega_\text{tot} = 1.05$ being the boundary of the imposed Ω_tot interval. This shows that the regular polyhedral spaces suppress the CMB anisotropies on large angles stronger than the prism spaces.

A further class of spherical spaces are the lens spaces $L(p, q)$ which are homogeneous for $q = 1$ and inhomogeneous for $q > 1$. The CMB properties of the lens spaces are analysed systematically in the survey presented in [11], and some interesting sequences of lens spaces $L(p, q)$ are found. But their CMB suppression is less pronounced compared to the regular polyhedral spaces. Typical values are in the range $S/S_{\mathcal{S}^3} \simeq 0.5 \ldots 0.6$ [11].

Therefore, the question emerges whether other classes of multi-connected spherical spaces can do better. The next class are the so-called double action manifolds where the group elements are composed of a right- and a left-handed Clifford transformation belonging to homogeneous deck groups R and L. Choosing $L = Z_n$ as the cyclic subgroup of Clifford translations and the subgroup R as the binary dihedral group $D_p^\star$, leads to the double action manifolds $DZ(p, n) = \mathcal{S}^3 / \left(D_p^\star \times Z_n \right)$ to which this paper is devoted. Three further classes of double action manifolds can be generated by the binary polyhedral groups leading to $TZ(24, n) := \mathcal{S}^3 / \left(T^\star \times Z_n \right)$, $OZ(48, n) := \mathcal{S}^3 / \left(O^\star \times Z_n \right)$, and $IZ(120, n) := \mathcal{S}^3 / \left(I^\star \times Z_n \right)$. These three groups do not possess analytical expressions for their eigenmodes in terms of Wigner polynomials and require a separate numerical treatment. Their analysis is reserved to a future paper.

The CMB suppression of the double action manifolds $DZ(p, n)$ is compared with that of the lens spaces $L(p, q)$ in figure 8. Three spaces attract attention because they reveal a stronger CMB suppression than all studied lens and prism spaces. These are the double action manifolds $DZ(16, 3)$, $DZ(8, 3)$, and $DZ(20, 3)$. The smallest large-angle correlations are seen in $DZ(16, 3)$ at $\Omega_\text{tot} = 1.036$, where $S/S_{\mathcal{S}^3} \simeq 0.291$ is reached. Although this suppression is remarkable, it is nevertheless less pronounced than that found in the regular polyhedral spaces.

Besides the three classes $TZ(24, n)$, $OZ(48, n)$, and $IZ(120, n)$, there are linked action manifolds [8] that are not analysed with respect to their CMB suppression until now. Except for these unexplored cases, one can summarise that the regular polyhedral spaces are the most promising spherical spaces with respect to their CMB suppression followed by some members of the class of double action manifolds $DZ(p, n)$, notably the spaces $DZ(16, 3)$, $DZ(8, 3)$, and $DZ(20, 3)$.

Acknowledgements

used in this work.

References

[1] G. Hinshaw *et al.*, Astrophys. J. Lett. **464**, L25 (1996).

[2] D. N. Spergel *et al.*, Astrophys. J. Supp. **148**, 175 (2003), astro-ph/0302209.

[3] M. Lachièze-Rey and J.-P. Luminet, Physics Report **254**, 135 (1995).

[4] J.-P. Luminet and B. F. Roukema, Topology of the Universe: Theory and Observation, in *NATO ASIC Proc. 541: Theoretical and Observational Cosmology*, p. 117, 1999, astro-ph/9901364.

[5] J. Levin, Physics Report **365**, 251 (2002).

[6] M. J. Rebouças and G. I. Gomero, Braz. J. Phys. **34**, 1358 (2004), astro-ph/0402324.

[7] J.-P. Luminet, The Shape and Topology of the Universe, in *Proceedings of the conference "Tessellations: The world a jigsaw", Leyden (Netherlands), March 2006*, 2008, arXiv:0802.2236 [astro-ph].

[8] E. Gausmann, R. Lehoucq, J.-P. Luminet, J.-P. Uzan, and J. Weeks, Class. Quantum Grav. **18**, 5155 (2001).

[9] R. Aurich, P. Kramer, and S. Lustig, Physica Scripta **84**, 055901 (2011), arXiv:1107.5214 [astro-ph.CO].

[10] P. Aurich, R. and S. Lustig, (2012), arXiv:1201.6490 [astro-ph.CO].

[11] P. Aurich, R. and S. Lustig, (2012), arXiv:1203.4086 [astro-ph.CO].

[12] S. Lustig, *Mehrfach zusammenhängende sphärische Raumformen und ihre Auswirkungen auf die Kosmische Mikrowellenhintergrundstrahlung*, PhD thesis, Universität Ulm, 2007, Verlag Dr. Hut, München (2007).

[13] A. R. Edmonds, *Angular momentum in quantum mechanics* (Princeton University Press, Princeton, 1957).

[14] J. Weeks, J.-P. Luminet, A. Riazuelo, and R. Lehoucq, Mon. Not. R. Astron. Soc. **352**, 258 (2004), astro-ph/0312312.

[15] B. Gold *et al.*, Astrophys. J. Supp. **192**, 15 (2011), arXiv:1001.4555 [astro-ph.GA].

[16] R. Aurich, H. S. Janzer, S. Lustig, and F. Steiner, Class. Quantum Grav. **25**, 125006 (2008), arXiv:0708.1420 [astro-ph].